Energetics of Homogeneous Intermolecular Vinyl and Allyl Carbon−Hydrogen Bond Activation by the 16-Electron Coordinatively Unsaturated Organometallic Fragment [Tp′Rh(CNCH$_2$CMe$_3$)]

Douglas D. Wick and William D. Jones*

Department of Chemistry, University of Rochester, Rochester, New York 14627

Received October 1, 1998

Reaction of the complex Tp′Rh(CNneo)(CH=CH$_2$)Cl (neo = CH$_2$CMe$_3$, Tp′ = hydridotris-(3,5-dimethylpyrazolyl)borate) with Cp$_2$ZrH$_2$ leads to the formation of Tp′Rh(CNneo)(CH=CH$_2$)H. This complex is also formed upon photolysis of a solution of Tp′Rh(CNneo)(PhN=C=Nneo) containing ethylene or by thermal reaction of Tp′Rh(CNneo)(c-hexyl)H with ethylene. The vinyl hydride complex rearranges to the more stable η^2-ethylene complex with a half-life of 8 h at 22 °C. Photolysis of a solution of Tp′Rh(CNneo)(PhN=C=Nneo) in liquid propylene produces the allylic activation product Tp′Rh(CNneo)(CH$_2$CH=CH$_2$)H, which rearranges ($t_{1/2}$ = 3 days at 22 °C) to the η^2-propylene complex. Allylic activation is also seen with isobutylene, but loss of olefin is observed at 22 °C in benzene solution to generate Tp′Rh(CNneo)(Ph)H ($t_{1/2}$ = 16.6 h). Photolysis of a *tert*-butylethylene solution of Tp′Rh-(CNneo)(PhN=C=Nneo) produces the trans vinyl hydride complex, which loses *tert*-butylethylene to generate Tp′Rh(CNneo)(Ph)H ($t_{1/2}$ = 113 days at 22 °C). A combination of kinetic selectivity and reductive elimination experiments have allowed for calculation of relative Rh−C bond strengths for both the rhodium allyl and vinyl hydride complexes and for the inclusion of these new data in an analysis of bond strength correlations. The results show that the trend for relative Rh−C bond strengths parallels the trend of hydrocarbon C−H bond strengths, i.e., Rh−Ph > Rh−vinyl > Rh−methyl > Rh−alkyl (1°) > Rh−cycloalkyl (2°) > Rh−benzyl > Rh−allyl, but that differences in M−C bond strengths typically exceed the differences in C−H bond strengths.

Introduction

One of the 10 most challenging unsolved problems for the catalysis research community is the development of an oxidation catalyst for the selective oxidation of methane, the primary component of natural gas, to methanol.[1] This challenge may be generalized to developing homogeneous transition-metal catalysts that activate and functionalize C−H bonds of alkanes for both industrial and synthetic applications. While the goal of catalytic activation and functionalization of hydrocarbons has been achieved with limited success in homogeneous systems,[2] heterogeneous systems still form the underpinning of commercial processes which are catalytic.[3a]

Crucial to the development of a viable homogeneous catalyst is a thorough understanding of the origin of the selectivities, both kinetic and thermodynamic, exhibited by reagents which activate C−H bonds. Ultimately, a rationally designed catalyst should be able to attack one type of C−H bond in preference to others and be able to generate a functionalized product from a hydrocarbon without the product reacting faster than the parent hydrocarbon.[3b]

While a number of homogeneous systems are known to stoichiometrically activate C−H bonds,[4] few have allowed for quantification of activated products crucial to the assessment of selectivity. Of these few, the most relevant to the results presented here are those studied by Bergman,[5] Jones,[6] and Wolczanski.[7] The reactivity studied by Bergman and Jones is typified by oxidative addition of a C−H bond to a coordinatively unsaturated late-metal center (d^8 Rh and Ir), generating a relatively stable hydrocarbyl hydride species. For Wolczanski's studies, the mode of reactivity involves 1,2-C−H bond addition to imido functionalities of early-metal (Ti, Zr) electrophilic transients to generate d^0 alkyl amido species. Despite the disparate nature of these systems, a common theme in their respective analyses is the

(1) Roth, J. F. *Chem. Eng. News* **1993**, *71*(22), 27.

(2) (a) Shilov, A. E. In *Activation and Functionalization of Alkanes*; Hill, C. L., Ed.; Wiley-Interscience: New York, 1989; pp 1−26, and references therein. (b) Sen, A.; Lin, M.; Kao, L.; Hutson, A. C. *J. Am. Chem. Soc.* **1992**, *114*, 6385−6392. (c) Nakata, K.; Miyata, T.; Jintoku, T.; Kitani, A.; Taniguchi, Y.; Takaki, K.; Fujiwara, Y. *Bull. Chem. Soc. Jpn.* **1993**, *66*, 3755−3759. (d) Fujiwara, Y.; Jintoku, T.; Uchida, Y. *New J. Chem.* **1989**, *13*, 649−650. (e) Sakakura, T.; Sodeyama, T.; Sasaki, K.; Wada, K.; Tanaka, M. *J. Am. Chem. Soc.* **1990**, *112*, 7221−7228. (f) Sakakura, T., Tanaka, M. *J. Chem. Soc., Chem. Commun.* **1987**, 758−759. (g) Maguire, J. A.; Goldman, A. S. *J. Am. Chem. Soc.* **1991**, *113*, 6706−6708. (h) Lin, M.; Hogan, T. E.; Sen, A. *J. Am. Chem. Soc.* **1996**, *118*, 4575−4580. (i) Sen, A.; Benvenuto, M. A.; Lin, M.; Hutson, A. C.; Basickes, N. *J. Am. Chem. Soc.* **1994**, *116*, 998−1003. (j) Labinger, J. A.; Herring, A. M.; Lyon, D. K.; Luinstra, G. A.; Bercaw, J. E.; Horvath, I. T.; Eller, K. *Organometallics* **1993**, *12*, 895−905. (k) Xu, W.; Rosini, G. P.; Gupta, M.; Jensen, C. M.; Kaska, W. C.; Krogh-Jespersen, K.; Goldman, A. S. *Chem. Commun.* **1997**, 2273−2274.

(3) (a) Crabtree, R. H. *Chem. Rev.* **1995**, *95*, 987−1007. (b) Arndtsen, B. A.; Bergman, R. G.; Mobley, T. A.; Peterson, T. H. *Acc. Chem. Res.* **1995**, *28*, 154−162.

10.1021/om9808211 CCC: $18.00
Publication on Web 01/20/1999

dominant influence of M−C bond strengths on the reported selectivities.

Jones and Hessell have previously reported the selectivity of the fragment [Tp′Rh(CNneo)] (where neo = CH_2CMe_3 and Tp′ = hydridotris(3,5-dimethylpyrazolyl)borate) for arene and alkane C−H bonds,[6b] in which the selectivity of [Tp′Rh(CNneo)] was compared to that of [Cp*Rh(PMe_3)] and [Cp*Ir(PMe_3)]. In these systems a high-energy 16-electron fragment is generated by loss of a photolabile ligand or dihydrogen and rapidly inserts into the C−H bonds of the hydrocarbon solvent. The rapid rate of C−H bond activation indicates that the kinetic barrier for this process is small, which in turn suggests little or no kinetic selectivity of the fragment. However, the rhodium systems, especially the RhTp′ system, distinguish themselves by a strong preference for aryl C−H bonds over alkyl C−H bonds and primary C−H bonds over secondary C−H bonds of normal alkanes (no secondary C−H activated products have been observed for complexes of rhodium).[6] Kinetic selectivity experiments have established the following relative (to benzene) trend for C−H bond preferences of [Tp′Rh(CNneo)]: Ph−H ≈ benzyl−H > Me−H > alkyl−H (1°) ≫ cycloalkyl−H.[6b]

Alkane σ-complexes[8] and arene π-complexes are undoubtedly involved as transient intermediates in these systems, but it should be pointed out that the presence of these species along the reaction coordinate does not affect the overall thermodynamics of the reactions. Substantial evidence has been presented for the existence of alkane σ-complexes prior to alkane activation, and such species may be important for understanding activation selectivities.[4k,9] An alkane σ-complex has even been observed spectroscopically at low temperature.[10]

Thermochemical, thermodynamic, and kinetic methods for measuring absolute or relative M−C bond strengths have been only recently available.[11,12] Thermodynamic studies of organometallic systems which mediate C−H activation by oxidative addition are

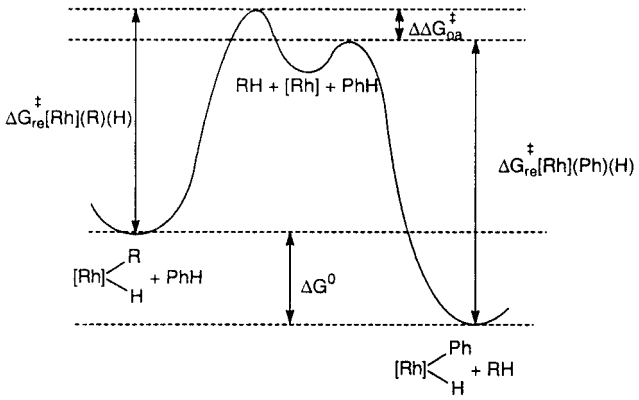

Figure 1. Reaction coordinate diagram for the equilibration of the phenyl hydride complex Tp′Rh(CNneo)(Ph)H and Tp′Rh(CNneo)(R)H, where R = alkyl, aryl, vinyl, and allyl, in a mixture of benzene and RH.

few[11,1314] and support the notion that metal−aryl bonds are much stronger than metal−alkyl bonds. Direct measurement of the equilibrium shown in eq 1 is not

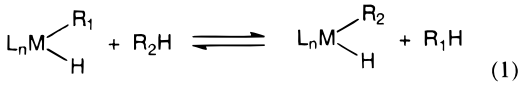

(1)

possible for complexes of the type Tp′Rh(CNneo)(R)H, made from photolysis of the carbodiimide complex[15] Tp′Rh(CNneo)(PhN=C=Nneo) in hydrocarbon solutions. The aromatic C−H bonds of *N*-phenyl-*N*′-neopentylcarbodiimide, which remains in solution after photolysis, are easily activated, which prevents measurement of only the solvent C−H activated species. However, Jones and Hessell have previously reported relative thermodynamic preferences of [Tp′Rh(CNneo)] for a number of hydrocarbon C−H bonds via an indirect measurement of the free energy of reaction using the kinetic parameters outlined in Figure 1 and eq 2. In this

$$\Delta G^\circ = \Delta G_{re}^{\ddagger}([Rh](Ph)(H)) + \Delta\Delta G_{oa}^{\ddagger}(RH) - \Delta G_{re}^{\ddagger}([Rh](R)(H)) \quad (2)$$

analysis, kinetic selectivities ($\Delta\Delta G_{oa}^{\ddagger}$) can be combined with free energies of reductive elimination of RH ($\Delta G_{re}^{\ddagger}$) to give relative free energies (ΔG°) for the complexes Tp′Rh(CNneo)(R)H.[16] Also, the presence of alkane σ-complexes and arene π-complexes is not explicitly shown in Figure 1, as these do not affect this thermodynamic analysis. The combination of the enthalpic term with the difference in C−H bond strengths yields relative M−C bond strengths. A plot of relative M−C bond strengths (solution phase) to C−H bond strengths (gas

(4) (a) Green, M. L. H.; O'Hare, D. *Pure Appl. Chem* **1985**, *57*, 1897−1910 and references therein. (b) Seidler, P. F.; Wenzel, T. T.; Bergman, R. G. *J. Am. Chem. Soc.* **1985**, *107*, 4358−4359. (c) Werner, H.; Hohn, A.; Dziallas, M. *Angew. Chem., Int. Ed. Engl.* **1986**, *25*, 1090−1092. (d) Desrosiers, P. F.; Shinomoto, R. S.; Flood, T. C. *J. Am. Chem. Soc.* **1986**, *108*, 7964−7970. (e) Baker, M. V.; Field, L. S. *J. Am. Chem. Soc.* **1987**, *109*, 2825−2826. (f) Hackett, M.; Whitesides, G. M. *J. Am. Chem. Soc.* **1988**, *110*, 1449−1462. (g) Ghosh, C. K.; Rodgers, D. P. S.; Graham, W. A. G. *J. Chem. Soc., Chem. Commun.* **1988**, 1511−1512. (h) Ghosh, C. K.; Graham, W. A. G. *J. Am. Chem. Soc.* **1989**, *111*, 375−376. (i) Ghosh, C. K.; Hoyano, J. K.; Krentz, R.; Graham, W. A. G. *J. Am. Chem. Soc.* **1989**, *111*, 5480−5481. (j) Barrientos, C.; Ghosh, C. K.; Graham, W. A. G.; Thomas, M. J. *J. Organomet. Chem.* **1990**, *394*, C31−C34. (k) Arndtsen, B. A.; Bergman, R. G. *Science* **1995**, *270*, 1970−1973. (l) Wang, C.; Ziller, J. W.; Flood, T. C. *J. Am. Chem. Soc.* **1995**, *117*, 1647−1648. (m) Wick, D. D.; Goldberg, K. I. *J. Am. Chem. Soc.* **1997**, *119*, 10235−10236. (n) Ghosh, C. K.; Hoyano, J. K.; Krentz, R.; Graham, W. A. G. *J. Am. Chem. Soc.* **1987**, *109*, 4726−4727. (o) Shilov, A. E.; Shul′pin, G. B. *Chem. Rev.* **1997**, 28799-2932.

(5) (a) Janowicz, A. H., Bergman, R. G. *J. Am. Chem. Soc.* **1983**, *105*, 3929−3939. (b) Periana, R. A.; Bergman, R. G. *Organometallics* **1984**, *3*, 508−510.

(6) (a) Jones, W. D.; Feher, F. J. *Acc. Chem. Res.* **1989**, *22*, 91−100. (b) Jones, W. D., Hessell, E. T. *J. Am. Chem. Soc.* **1993**, *115*, 554−562.

(7) Schaller, C. P.; Cummins, C. C.; Wolczanski, P. T. *J. Am. Chem. Soc.* **1996**, *118*, 591−611 and references therein. Bennett, J. L.; Wolczanski, P. T. *J. Am. Chem. Soc.* **1997**, *119*, 10696−10719.

(8) Hall, C.; Perutz, R. N. *Chem. Rev.* **1996**, *96*, 3125−3146.

(9) Gross, C. L.; Girolami, G. S. *J. Am. Chem. Soc.* **1998**, *120*, 6605−6606.

(10) Geftakis, S.; Ball, G. E. *J. Am. Chem. Soc.* **1998**, *120*, 9953−9954.

(11) Martinho-Simões, J. A.; Beauchamp, J. L. *Chem. Rev.* **1990**, *90*, 629−688.

(12) (a) Halpern, J. *Acc. Chem. Res.* **1982**, *15*, 238−244. (b) Marks, T. J. *Polyhedron* **1988**, *7*, 1406−1637 (Symposia in Print).

(13) Buchanan, J. M.; Stryker, J. M.; Bergman, R. G. *J. Am. Chem. Soc.* **1986**, *108*, 1537−1550.

(14) Nolan, S. P.; Hoff, C. D.; Stoutland, P. O.; Newman, L. J.; Buchanan, J. M.; Bergman, R. G.; Yang, G. K.; Peters, K. S. *J. Am. Chem. Soc.* **1987**, *109*, 3143−3145.

(15) Hessell, E. T.; Jones, W. D. *Organometallics* **1992**, *11*, 1496−1505.

(16) In calculations of this type entropies and solvation energies for the various metal alkyl and aryl hydride complexes are assumed to be equal. Thus, these terms cancel in the calculation of energy differences, and the free energy of reaction is then approximately equal to the enthalpy of reaction.

phase) can be made which, given an error in bond strengths of ±1−2 kcal/mol, is nearly linear (see Supporting Information or Figure 5 of ref 6b). A plot of this type allows for prediction of unknown M−C bond strengths based on known C−H bond strengths. In comparison, Bryndza and co-workers have shown linear 1:1 relationships between M−X and H−X bond strengths for two different systems, $Cp^*Ru(PMe_3)_2(X)$ and (dppe)Pt(Me)(X), where X is OH, OR, NR_2, PR_2, SiR_3, and SH.[17] These correlations appear to be unaffected by steric differences.

The driving force for addition of a C−H bond to a coordinatively unsaturated transition-metal fragment lies in the formation of M−H and M−C bonds whose combined bond dissociation energies (BDE) exceed the BDE of the starting alkane C−H bond. Halpern has previously suggested that maximizing this driving force rests with maximizing the M−C bond strengths, since M−H bond strengths are typically invariant for later first row transition metals (∼65 kcal/mol).[18] Halpern has further indicated that the key to maximizing M−C bond strengths is minimizing steric encroachment, a view supported by the effect of steric bulk being greater than that of electronics on the Co−R BDE's in complexes of the type Co(SALOPH)(py)(R) and $Co(DH)_2(L)(R)$.[19] However, a full understanding of the effect of metal oxidation state and ligand set on M−C and M−H BDE's has yet to be achieved.[20]

Wolczanski and co-workers have studied hydrocarbon activation via 1,2-RH elimination from several early-transition-metal hydrocarbyl complexes. They have found that transition-state energy differences are significantly more important than ground-state energy differences for 1,2-RH elimination from $(t\text{-}Bu_3SiNH)_2Ta(t\text{-}Bu_3SiN)(R)$, where R = Me, Ph, Bz, and $CH_2(t\text{-Bu})$, and $(^tBu_3SiNH)_3Zr(R)$, where R = c-Pr, Ph, Bz, Ar, and Me.[21] For these complexes they find that the difference in M−C bond strengths are of the same order of magnitude as the difference in the corresponding C−H bond strengths, as in the Bryndza−Bercaw study.[17] Thus, the discriminating ability of a putative Ta or Zr d^0 imido intermediate is attributed to kinetic selectivity and not to thermodynamic selectivity. These results are in contrast with the work of Hessell and Jones, in which the ground-state energy differences between alkyl and aryl hydride complexes of rhodium dominate the reactivity. In these latter studies, the difference in M−C bond strengths is *larger* than the corresponding difference in C−H bond strengths, giving rise to a strong thermodynamic preference for cleaving strong C−H bonds in these electron-rich late-transition-metal complexes.[6b]

More recent studies by Wolczanski with a series of $(^tBu_3SiO)_2(^tBu_3SiNH)TiR$ compounds allowed determination of the relative thermodynamic stability of some 15 derivatives.[22] In contrast to the earlier studies with Zr and Ta, these data show a correlation between D(Ti−R) and D(H−R) in which the differences in titanium−carbon bond strengths are substantially greater than the differences in carbon−hydrogen bond strengths, in agreement with the Hessell−Jones conclusions.

While the interpretation of these types of correlations is important, the available data on metal−carbon bond strengths are still wanting. Conspicuously absent from the [Tp′Rh(CNneo)] series are Rh−vinyl and Rh−allyl species. It is known that vinyl hydrides of $(C_5Me_5)Rh$, $(C_5Me_5)Ir$, and $(dmpe)_2Fe$ are less stable than their η^2-olefin isomers.[23] Two examples are known in which a vinyl hydride complex is more stable than its η^2-ethylene isomer, $Ir(HBPf_3)(CO)(C_2H_3)H$[4i] (where $HBPf_3$ is hydridotris(3-(trifluoromethyl)-5-methyl-1-pyrazolyl)-borate) and $Tp'IrL(C_2H_3)H$ (where L = PMe_3 or PMe_2-Ph).[24] In this report, further reactivity of the Tp′ fragment [Tp′Rh(CNneo)] with ethylene, propylene, isobutylene, and *tert*-butylethylene is examined. The reactions involving the last two substrates allow for the characterization of two unusually stable complexes, the allyl hydride $Tp'Rh(CNneo)(CH_2CMe{=}CH_2)H$ (**5**) and the vinyl hydride $Tp'Rh(CNneo)(HC{=}CHCMe_3)H$ (**6**). Kinetic experiments are used to calculate the enthalpy difference between each complex and the phenyl hydride complex Tp′Rh(CNneo)(Ph)H. In turn, these enthalpy differences can be combined with differences in C−H bond strengths for benzene and the olefin to estimate relative Rh−vinyl and Rh−allyl bond strengths. The resulting trend, Rh−Ph ≫ Rh−vinyl > Rh−Me > Rh−alkyl (1°) > Rh−cycloalkyl > Rh−Bz > Rh−allyl,[6b] follows the previously proposed trend based on early studies with the $(C_5Me_5)Rh(PMe_3)(R)H$ complexes, i.e., M−Ph ≫ M−vinyl, M−Me > $M-CH_2R$ > $M-CHR_2$ > M−Bz.[6a,25] Full characterization of the vinyl species as its chloride analogue, $Tp'Rh(CNneo)(CH{=}CHCMe_3)Cl$ (**6-Cl**), is also presented.

Results and Discussion

Preparation and Characterization of Rhodium Tris(pyrazolyl)borate Vinyl Hydride and Ethylene Complexes. The vinyl hydride complex $Tp'Rh(CNneo)(CH{=}CH_2)H$ (**1**; neo = CH_2CMe_3), can be prepared by two methods, as depicted in Scheme 1. The reaction of the vinyl chloride complex with Cp_2ZrH_2 in benzene gives **1** in quantitative yield. The vinyl hydride can be isolated by flash chromatography through silica gel. Substantially lower yields (20%) of **1** are obtained from photolysis of $Tp'Rh(CNneo)(PhN{=}C{=}Nneo)$ in cyclohexane under 2 atm of ethylene at 22 °C for 1 h.

The ^1H NMR spectrum of **1** in C_6D_6 shows a doublet at δ −13.982 for the rhodium-bound hydride ligand. The hydride resonance of **1** is at higher field than that of

(17) Bryndza, H. E.; Fong, L. K.; Paciello, R. A.; Tam, W.; Bercaw, J. E. *J. Am. Chem. Soc.* **1987**, *109*, 1444−1456.
(18) Halpern, J. *Inorg. Chim. Acta* **1985**, *100*, 41−48.
(19) Ng, F. T. T.; Rempel, G. L.; Halpern, J. *Inorg. Chim. Acta* **1983**, *77*, L165
(20) For a review see: Davies, J. A.; Watson, P. L.; Liebman, J. F.; Greenberg, A. *Selective Hydrocarbon Activation*; VCH: New York, 1990; pp 149−206.
(21) (a) Schaller, C. P.; Cummins, C. C.; Wolczanski, P. T. *J. Am. Chem. Soc.* **1996**, *118*, 591−611 and references therein. (b) Schaller, C. P.; Wolczanski, P. T. *Inorg. Chem.* **1993**, *32*, 131−144.
(22) Bennett, J. L.; Wolczanski, P. T. *J. Am. Chem. Soc.* **1997**, *119*, 10697−10719.
(23) (a) Jones, W. D.; Feher, F. J. *J. Am. Chem. Soc.* **1984**, *106*, 1650−1663. (b) Wenzel, T. T.; Bergman, R. G. *J. Am. Chem. Soc.* **1986**, *108*, 4856−4867. (c) Baker, M. V.; Field, L. D. *J. Am. Chem. Soc.* **1986**, *108*, 7433−7434. (d) Baker, M. V.; Field, L. D. *J. Am. Chem. Soc.* **1986**, *108*, 7436−7438. (e) Bell, T. W.; Brough, S.-A.; Partridge, M. G.; Perutz, R. N.; Rooney, D. *Organometallics* **1993**, *12*, 2933−2941.
(24) Gutiérrez-Puebla, E.; Monge, Á.; Nicasio, M. C.; Pérez, P. J.; Poveda, M. L.; Rey, L.; Ruíz, C.; Carmona, E. *Inorg. Chem.* **1998**, *37*, 4538−4546.
(25) Jones, W. D. In *Activation and Functionalization of Alkanes*; Hill, C. L., Ed.; Wiley: New York, 1989; pp 111−149.

Scheme 1

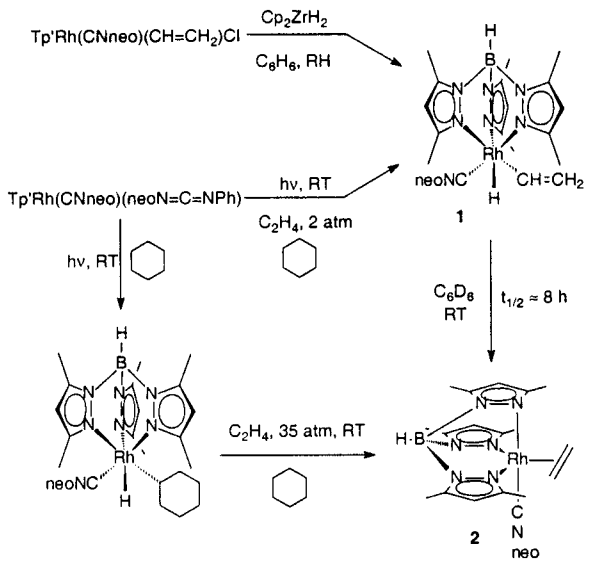

Tp′Rh(CNneo)(C_6H_5)H (δ −13.650) and at lower field than that of Tp′Rh(CNneo)(CH_3)H (δ −14.846). The resonances for the methyl groups and methine protons of the Tp′ ligand appear as nine singlets in a 3:3:3:3:3:3:1:1:1 ratio from δ 2.2 to 5.8. This pattern indicates that the three pyrazolyl rings of the Tp′ ligand are inequivalent due to chirality at rhodium. The resonance for the proton attached to the rhodium-bound carbon of the vinyl ligand (H_α) appears as a doublet of doublets of doublets at δ 7.747 with $J_{trans-HH}$ = 18 Hz, J_{cis-HH} = 10 Hz, and $^2J_{RhH}$ = 3 Hz. The resonances of the geminal vinyl protons (H_β) appear as a doublet of triplets of doublets at δ 6.210 (J_{cis-HH} = 10 Hz, $J_{gem-HH} = {}^3J_{RhH}$ = 3 Hz, $^4J_{H-hydride}$ (J_w) = 2 Hz) and a doublet of triplets at δ 5.753 ($J_{trans-HH}$ = 18 Hz, $J_{gem-HH} = {}^3J_{RhH}$ = 3 Hz). The assignments of the vinyl ligand protons were confirmed by homonuclear decoupling experiments. The ^{1}H NMR spectral data support a description of **1** as an octahedral Rh(III) complex which contains a tridentate Tp′ ligand, as observed in the solid-state crystal structures for the cyclopropyl, isopropyl, and *n*-pentyl chloride complexes described previously.[6b,26]

In C_6D_6 at 22 °C the vinyl hydride complex cleanly converts to a new species, which has been identified as the Rh(I) ethylene complex Tp′Rh(CNneo)(η^2-C_2H_4) (**2**). The half-life for this process is approximately 8 h at 22 °C (Scheme 1). The phenyl-d_5 deuteride complex is the only additional product, accounting for ∼5% of the total yield by NMR spectroscopy. This result indicates that reductive elimination to produce free ethylene followed by recoordination does not occur. Since there is a large excess of benzene, the 16-electron intermediate [Tp′Rh(CNneo)] would activate benzene preferably to coordinating ethylene under the conditions of the experiment (*vide infra*). The isomerization of **1** to **2** is therefore intramolecular. Under a high pressure of ethylene in a bomb reactor the cyclohexyl hydride complex (made from photolysis of a cyclohexane solution of Tp′Rh(CNneo)(PhN=C=Nneo)) can be fully converted to **2** in 24 h (Scheme 1).

A comparison of the ^{1}H NMR spectra of **2** and **1** shows the resonance for the neopentyl moiety of the isocyanide ligand of **2** at higher field than that of **1**, δ 0.504 and 0.641, respectively. The ^{1}H NMR spectrum of **2** in C_6D_6 shows two broad doublets of doublets at δ 2.512 and 3.385 in a 1:1 ratio for the bound ethylene protons, indicating that ethylene rotation is hindered. The larger coupling constant of 8 Hz is assigned as a *cis* coupling constant, with the smaller coupling constant of 2 Hz being assigned as a *gem* coupling. Four singlets in a 1:1:2:2 ratio between δ 2.2 and 2.6 and two singlets in a 1:2 ratio between δ 5.3 and 5.9 are observed at ambient temperature, which indicate that two of the three pyrazolyl rings of the Tp′ ligand are equivalent. The resonance for the isocyanide methylene protons appears as a singlet, not an AB quartet as is observed for the alkyl chloride complexes,[26] which indicates the equivalence of these two protons. The 2:1 symmetry of the Pz′ rings of **2** is observed down to −78 °C in THF-d_8.

The structure of **2** is assigned as a trigonal bipyramid with an axial isocyanide ligand and the ethylene lying in the equatorial plane[27] on the following basis. First, an X-ray structure of the related derivative (η^3-Tp′)Rh(CN-2,6-xylyl)(C_2H_4) shows this coordination geometry.[28] Second, the ^{11}B{^{1}H} NMR spectrum of **2** displays a broad singlet at δ −9.38 (*cf.* δ −9.28 for (η^3-Tp′)Rh(CN-2,6-xylyl)(C_2H_4)), a chemical shift which is indicative of η^3-Tp′ coordination.[29] Third, the infrared spectrum of **2** shows ν_{B-H} at 2523 cm^{-1} (*cf.* 2525 cm^{-1} for (η^3-Tp′)Rh(CN-2,6-xylyl)(C_2H_4)), again indicating η^3-Tp′ coordination.[30] By comparison, the related complexes Tp′Rh(CNR)$_2$ (R = 2,6-xylyl and neopentyl) have been structurally characterized as η^2-Tp′ complexes,[31] and all display ν_{B-H} values of less than 2500 cm^{-1} in KBr and in solution. Finally, a number of other tbp Tp complexes with olefin ligands are known and display NMR data similar to those for **2**.[32]

Compound **2** serves as a poor thermal precursor of [Tp′Rh(CNneo)] for C−H activation but as an excellent photochemical one. Reaction between **2** and C_6D_6 at 58 °C showed only 10% conversion of **2** to Tp′Rh(CNneo)(C_6D_5)D after 2 days with concomitant loss of ethylene. In contrast, conversion of **2** to Tp′Rh(CNneo)(C_6D_5)D and free ethylene is complete after a C_6D_6 solution of **2** is irradiated (λ >345 nm) for only 10 min at 22 °C.

Preparation and Characterization of Rhodium Tris(pyrazolyl)borate Allyl Hydride and η^2-Olefin Complexes. The allyl hydride complex Tp′Rh(CNneo)(CH_2CH=CH_2)H (**3**) can be prepared by photolysis of Tp′Rh(CNneo)(PhN=C=Nneo) in neat propylene at −78 °C (Scheme 2). Replacement of propylene solvent by C_6D_6 allows observation of a doublet at δ −14.783 for the hydride ligand of **3** in the ^{1}H NMR spectrum, similar

(26) Wick, D. D.; Jones, W. D. *Inorg. Chem.* **1997**, *36*, 2723−2729.
(27) Albright, T. A.; Hoffman, R.; Thibeault, J. C.; Thorn, D. C. *J. Am. Chem. Soc.* **1979**, *101*, 3801−3812.
(28) Wick, D. D.; Northcutt, T. O.; Lachicotte, R. J.; Jones, W. D. *Organometallics* **1998**, *17*, 4784−4794.
(29) Northcutt, T. O.; Lachicotte, R. J.; Jones, W. D. *Organometallics* **1998**, *14*, 5148−5152.
(30) Akita, M.; Ohta, K.; Takahashi, Y.; Hikichi, S.; Moro-oka, Y. *Organometallics* **1997**, *16*, 4121−4128.
(31) Jones, W. D.; Hessell, E. T. *Inorg. Chem.* **1991**, *30*, 778−783.
(32) (a) Cocivera, M.; Ferguson, G.; Branko, K.; Lalor, F. J.; O'Sullivan, D. J.; Parvez, M.; Ruhl, B. *Organometallics* **1982**, *1*, 1132−1139. (b) Cocivera, M.; Ferguson, G.; Lalor, F. J.; Szczecinski, P. *Organometallics* **1982**, *1*, 1139−1142. (c) Ciriano, M. A.; Fernández, M. J.; Modrego, J.; Rodríguez, M. J.; Oro, L. A. *J. Organomet. Chem.* **1993**, *443*, 249−252. (d) Clark, H. C.; Manzer, L. E. *Inorg. Chem.* **1974**, *13*, 1291−1297. (e) Manzer, L. E.; Meakin, P. Z. *Inorg. Chem.* **1976**, *15*, 3117−3120. (f) Bucher, U. E.; Currao, A.; Nesper, R.; Rüegger, H.; Venanzi, L. M.; Younger, E. *Inorg. Chem.* **1995**, *34*, 66−74.

Scheme 2

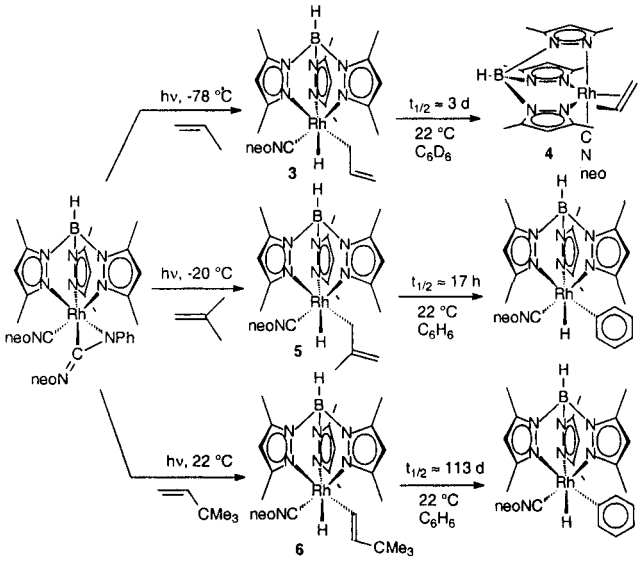

to other alkyl hydride complexes.[6b] This resonance is substantially upfield of the hydride resonance of **1** and indicates that the methyl C−H bond of propylene, not a vinyl proton, has been activated (*cf.* Tp′Rh(CNneo)-$(CH_3)H$ at δ −14.846). The chiral nature of the rhodium center and η^3-Tp′ coordination are indicated by the observation of three resonances between δ 5.6 and 5.8 for the methine protons of the Tp′ ligand. A complete ^{1}H NMR characterization of this complex was not possible due to overlapping resonances of free carbodiimide and carbodiimide activated products and residual propylene.

The allyl hydride **3** is thermally unstable and is observed to rearrange to the known Rh(I) propylene complex Tp′Rh(CNneo)(η^2-MeCH=CH_2) (**4**) with an approximate half-life of 3 days at 22 °C in C_6D_6 (Scheme 2).[28] The resonance of the neopentyl moiety of the isocyanide ligand of **4** shifts upfield to that of **3**, as observed in the previous rearrangement of the vinyl hydride complex to the ethylene complex. The chiral nature of the rhodium and inequivalence of the pyrazolyl rings is also maintained, as shown by the appearance of three new resonances in the region between δ 5.2 and 6 during the isomerization process. The structure of **3** has been assigned to be trigonal bipyramidal with an η^3-Tp′ ligand on the basis of IR (ν_{B-H} = 2523 cm^{-1}) and ^{11}B NMR (δ −9.13) spectroscopy.[29] A chiral rhodium center is generated by the coordination of propylene, which removes the plane of symmetry in a trigonal-bipyramidal structure as observed for the coordination of ethylene.

Due to the formation of small quantities of additional side products, it was difficult to ascertain if more than one rotamer of **4** was formed. Minor resonances are seen in the ^{1}H NMR spectrum that are consistent with the presence of a small amount of a second propylene rotamer (see Experimental Section). Ghosh and Graham observed similar results with the rearrangement of Tp′Rh(CO)(CH_2CH=CH_2)H to Tp′Rh(CO)(η^2-MeCH=CH_2).[33]

The methallyl hydride complex Tp′Rh(CNneo)(CH_2-CMe=CH_2)H (**5**) was prepared by photolysis of Tp′Rh-(CNneo)(PhN=C=Nneo) in neat isobutylene at −20 °C (Scheme 2). The ^{1}H NMR spectrum of **5** in C_6D_6 displays a doublet resonance for the hydride ligand at δ −14.661 which is consistent with allylic C−H bond activation rather than vinylic C−H bond activation. The resonance for H_α of the σ-methallyl ligand appears as an AB quartet of doublets at δ 3.094. This pattern indicates that the methylene protons are diastereotopic and are coupled to rhodium (J_{RhH} = 4 Hz). The methyl group and the geminal vinyl protons of the allyl ligand appear as a singlet at δ 2.171 and two multiplets between δ 4.9 and 5.2, respectively. In C_6H_6, isomerization to an olefin complex does not occur. Instead, **5** slowly reductively eliminates isobutylene and activates C_6H_6. This is a good example of a relatively stable allyl hydride complex containing a [Tp′RhL] fragment. The reductive elimination of isobutylene from **5** in C_6H_6 at 22 °C is first-order through 3 half-lives (Figure 2). The rate constant is [1.16(5)] × 10^{-5} s^{-1}, which corresponds to a half-life of 16.6(7) h.

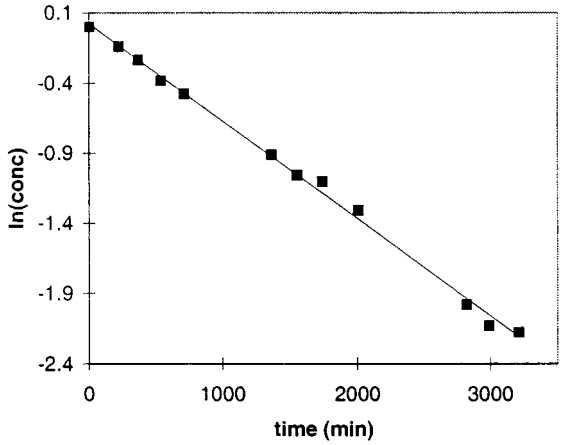

Figure 2. Plot of ln[**5**] vs time for the reductive elimination of isobutylene from Tp′Rh(CNneo)($CH_2C(CH_3)$=CH_2)H (**5**) in C_6H_6 at 22 °C.

The above observation indicates that the steric bulk of an olefin can prevent the formation of a stable η^2-olefin complex. It was thought that selective activation of a *vinyl* proton to yield a stable vinyl C−H bond activation product that would not isomerize to an η^2-olefin complex might therefore be feasible with the proper choice of olefin. It is known that the fragments [Tp′Rh(CNneo)] and [Tp′Rh(CO)] do not activate the C−H bonds of neopentane, presumably due to substantial kinetic and thermodynamic barriers brought about by severe steric interactions of the substrate and the fragment.[6b] This conclusion suggests that the bulky *tert*-butyl group of 3,3-dimethyl-1-butene (*tert*-butylethylene) would most likely direct the reactivity toward the less congested end of the olefin and also would prevent rearrangement of a vinyl hydride complex to an olefin complex.

Photolysis of Tp′Rh(CNneo)(PhN=C=Nneo) in neat *tert*-butylethylene gives exclusively the *trans*-3,3-dimethylbutenyl hydride species Tp′Rh(CNneo)(CH=$CHCMe_3$)H (**6**) (Scheme 2). In the ^{1}H NMR spectrum of **6** in C_6D_6 the hydride resonance appears as a doublet at δ −14.001, which is at lower field than that of the methallyl (**5**) or methyl hydride complexes and is comparable to that of the vinyl hydride complex **1**. A doublet of doublets at δ 5.850 is assigned to the vinyl

(33) Ghosh, C. K. Ph.D. Thesis, University of Alberta, Edmonton, AB, Canada, 1988.

proton attached to C_β of the *tert*-butylethenyl ligand. The larger coupling constant of 16 Hz attests to the *trans* relationship of the vinyl hydrogens. The smaller coupling constant of 2 Hz indicates coupling to rhodium through three bonds. The vinyl hydrogen attached to C_α was not observed due to overlapping resonances of free carbodiimide in solution. Formation of the least sterically crowded product has been previously observed for $V(RNH)_2(NR)$(*trans*-*tert*-butylethylene) prepared by the activation of *tert*-butylethylene by $V(RNH)_2(NR)(CH_3)$.[34] Also, H/D exchange in *tert*-butylethylene catalyzed by $Ir(PMe_3)_2H_5$ occurs selectively at the position *trans* to the *tert*-butyl group.[35] As for **5**, **6** does not rearrange to an olefin complex in C_6H_6 but rather reductively eliminates *tert*-butylethylene and activates benzene. The reductive elimination of *tert*-butylethylene from **6** in C_6H_6 at 22 °C is first-order through 3 half-lives with a rate constant of $[7.1(4)] \times 10^{-8}$ s^{-1}. This rate constant corresponds to a half-life of 113(6) days, which is substantially slower than the conversion of **1** to **2**.

The addition of CCl_4 to a hexanes solution of **6** at −20 °C results in the complete conversion of **6** to its chloride analogue, Tp′Rh(CNneo)(CH=CHCMe$_3$)Cl (**6-Cl**). Recrystallization from a hexanes solution of **6-Cl** at −20 °C yields pale brown-yellow air-stable crystals of analytical purity. The *tert*-butylethenyl chloride complex has been fully characterized by ^{1}H NMR, ^{13}C{^{1}H} NMR, and IR spectroscopy and elemental analysis. The two vinyl protons of the *tert*-butylethenyl ligand appear as a doublet at δ 5.913 (H_β) and a doublet of doublets at δ 7.159 (H_α) in the ^{1}H NMR spectrum of **6-Cl** in C_6D_6. The *trans* relationship of these two protons is confirmed by the observed coupling constant of 15 Hz. Homonuclear decoupling experiments support the assignments of H_α and H_β. All spectroscopic data are consistent with the description of **6-Cl** as an octahedral Rh(III) complex containing a tridentate Tp′ ligand.

The solid-state X-ray structure of **6-Cl** shown in Figure 3 is consistent with the structural conclusions made from the spectroscopic data. Selected bond angles and distances are listed in Table 1, with the remainder of the crystallographic data being contained in the Supporting Information. The structure has a slightly distorted octahedral geometry. The angles made by Rh−C16−C17 and C16−C17−C18 are both greater than 120°, which reflects the greater steric interaction between the neopentyl moiety of the *tert*-butylethenyl ligand and the methyl group of the proximal Tp′ pyrazolyl ring. Also reflective of the crowded coordination environment in **6-Cl** is the nearly linear neopentyl isocyanide CNC unit (176.9°). This angle also indicates that back-bonding by a rhodium d orbital to the CN π^* orbital is not operative due to the electron-poor nature of the rhodium (formally Rh(III); IR ν_{C-N} 2214 cm^{-1}).

Kinetic Selectivity Experiments. Having established the ^{1}H NMR characteristics of **5** and **6**, the kinetic selectivity of [Tp′Rh(CNneo)] for allyl and vinyl C−H bonds relative to phenyl C−H bonds was investigated. Competition studies were performed in which [Tp′Rh(CNneo)(PhN=C=Nneo)] was irradiated in a mixture

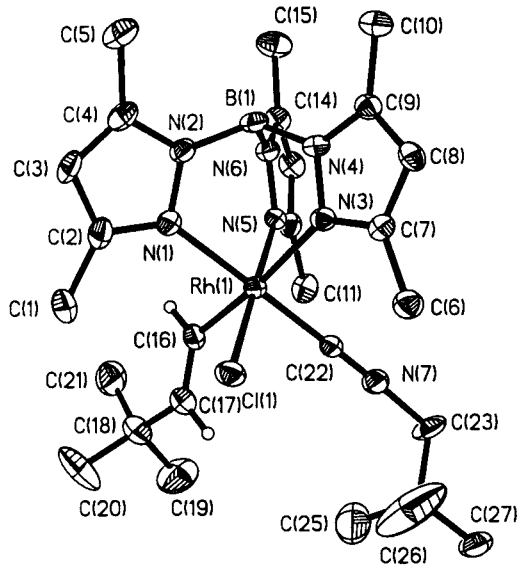

Figure 3. ORTEP drawing of Tp′Rh(CNneo)(CH=CHCMe$_3$)Cl **(6-Cl)**. Ellipsoids are shown at the 50% probability level. Hydrogen atoms (except those on the vinyl group) have been omitted for clarity.

Table 1. Selected Bond Angles (deg) and Distances (Å) for Tp′Rh(CNneo)(CH=CHCMe$_3$)Cl (6-Cl)

C17−C16−Rh	130.5(5)	C22−Rh−N3	93.1(2)
C18−C17−C16	127.2(6)	C22−Rh−N5	93.1(2)
C16−Rh−Cl	92.5(2)	N1−Rh−N3	86.8(2)
C16−Rh−C22	90.9(2)	N1−Rh−N5	88.2(2)
C16−Rh−N1	89.3(2)	N3−Rh−N5	87.1(2)
C16−Rh−N3	174.1(2)	C22−N7−C23	176.9(6)
C16−Rh−N5	88.3(2)	Cl−Rh−N1	91.6(1)
C22−Rh−Cl	87.0(2)	Cl−Rh−N3	92.1(1)
C22−Rh−N1	178.6(2)	Cl−Rh−N5	179.3(1)
C16−C17	1.299(7)	N7−C23	1.443(7)
Rh−C16	2.021(6)	Rh−N1	2.092(4)
Rh−Cl	2.352(2)	Rh−N3	2.209(5)
Rh−C22	1.910(6)	Rh−N5	2.045(4)
C22−N7	1.141(6)		

Table 2. Conditions and Results for Determining the Kinetic Selectivity of the Fragment [Tp′Rh(CNneo)] for Benzene Relative to *tert*-Butylethylene and Benzene Relative to Isobutylene

run no.	substrates	solvent ratio (V_1/V_2)	T (°C)	abs integral ratio (I_1/I_2)	k_{rel}
1	benzene/ *tert*-butylethylene	1:4	22	3.7:1.0	10:1
2	isobutylene/pentane	1:1	−15	1.1:1.0	1.1:1
3[6b]	benzene/pentane	1:2	−15	3.0:1.0	4.7:1

of two hydrocarbons. To ensure that this competition was purely kinetic in origin it was necessary that (1) the relative product ratios formed under kinetic control during photolysis did not change significantly over the time required to obtain a ^{1}H NMR spectrum of the products, (2) irradiation did not promote product interconversion, and (3) an approach to thermal equilibrium could be observed. Earlier selectivity studies have shown that the [Tp′Rh(CNneo)] fragment abided by the criteria above.[6b]

The experimental conditions for the selectivity of [Tp′Rh(CNneo)] for benzene vs *tert*-butylethylene and isobutylene vs pentane are listed in Table 2. Each run was reproducible, and the kinetic selectivities were

(34) Horton, A. D.; de With, J. *Angew. Chem., Int. Ed. Engl.* **1993**, *32*, 903−905.
(35) Faller, J. W.; Felkin, H. *Organometallics* **1985**, *4*, 1488−1490.

calculated on a per-molecule basis using eq 3 (where I = peak integration area, V = volume of hydrocarbon, d = density of hydrocarbon, and MW = molecular weight of hydrocarbon). In run 2 of Table 2 the products of the reaction were not observed directly in the substrate solution after photolysis due to the volatility of isobutylene. In this run, the solvent mixture was removed under vacuum at −78 °C and the residue was dissolved in THF-d_8 at −78 °C. The two products are stable under these conditions.

$$k_1/k_2 = (I_1/I_2)(V_2/V_1)(d_2/d_1)(\mathrm{MW}_1/\mathrm{MW}_2) \qquad (3)$$

Little preference of the coordinatively unsaturated fragment [Tp′Rh(CNneo)] is observed for C−H activation of an allyl C−H bond of isobutylene vs a primary C−H bond of *n*-pentane. The kinetic selectivity value for benzene vs isobutylene (4.3:1) is then similar to that for benzene vs *n*-pentane (4.7:1). This ratio corresponds to a small difference in the activation barriers to oxidative addition ($\Delta\Delta G_{oa}^{\ddagger}$(RH)) of 0.75 kcal/mol, which could reflect the ease of formation of σ-alkane complexes (for sp^3 C−H activation of pentane or isobutylene) vs an arene π-complex (for benzene activation) prior to C−H cleavage. The fragment [Tp′Rh(CNneo)] prefers activation of a benzene molecule vs a *tert*-butylethylene molecule by 10:1. The value of $\Delta\Delta G_{oa}^{\ddagger}$(RH) for this set of substrates is 1.35 kcal/mol. Even on a per-hydrogen basis activation of a phenyl C−H bond is favored over activation of the terminal *trans*-vinyl C−H bond by 1.7:1 (=10/1 × 1/6).

Thermodynamic Assessment. The data from the reductive elimination and kinetic selectivity studies can be combined to assess the thermodynamics of vinyl and allyl C−H bond activation for this system. The reductive eliminations might proceed through unstable η^2-olefin complexes, or the eliminations might occur directly without an intermediate complex. In either case, the lowest energy pathway for C−H activation by the 16-electron intermediate must also be the lowest energy pathway for olefin elimination, so that the thermodynamic analysis is independent of the mechanism. (The same argument applies to the intermediacy of alkane σ-complexes along the reaction coordinate.) Determination of the relative free energy ($\Delta G°$) of the complex **5** (or **6**) was accomplished by subtracting the free energy of reductive elimination for **5** (or **6**) from the sum of the free energy of reductive elimination of benzene and the difference in the free energies of activation between benzene and isobutylene (*tert*-butylethylene) (eq 2, Figure 4). Using eq 4 the C−H bond strength difference

$$D_{rel}(\mathrm{M{-}R}) = D(\mathrm{Rh{-}Ph}) - D(\mathrm{Rh{-}R}) = \Delta G° + D(\mathrm{Ph{-}H}) - D(\mathrm{R{-}H}) \qquad (4)$$

between benzene[36] and the substrate[37] can be combined with $\Delta G°$ to give the relative M−C bond strengths for the hydrocarbon ligands of **5** and **6**. In Table 3 the

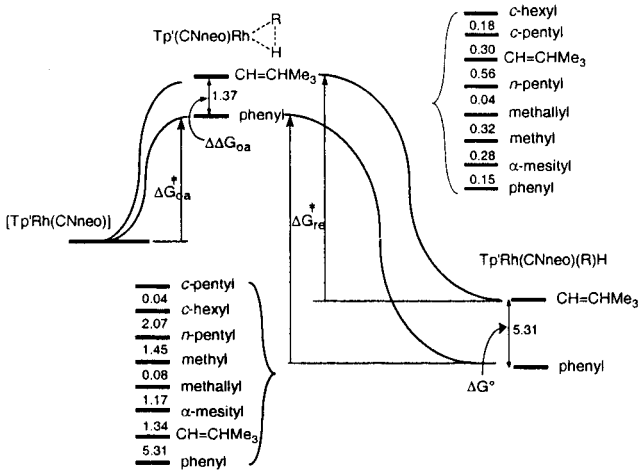

Figure 4. Summary of free energies (kcal/mol) for alkane and arene activation by [Tp′Rh(CNneo)].

selectivities and thermodynamics for the formation of **5** and **6** in addition to a number of alkanes and arenes previously studied by Jones and Hessell are summarized.[6b] All of the products in these reactions are d^6-octahedral Rh^{III} complexes of the type (η^3-Tp′)Rh(CNneo)(R)H, so that only small differences in metal reorganization energies are expected within this series. Other studies provide evidence, however, that these differences can be large when ligands of varied σ-donor/π-acceptor capability are compared.[38]

Figure 5 is a plot of the relative rhodium−carbon bond strengths for complexes of the type Tp′Rh(CNneo)(R)H vs the C−H bond strengths of the corresponding hydrocarbon (RH). Clearly, a linear relationship only loosely describes the relationship between C−H and M−C bond strengths. Nor is there a linear free energy relationship between $\Delta G^{\ddagger}_{oa}$ and $\Delta G°$ (see Supporting Information). The plot suggests that the rhodium−phenyl, rhodium−benzyl, and rhodium−methallyl bond strengths are strong, on the basis of the relative C−H bond strengths of benzene, mesitylene, and isobutylene (allylic), respectively. While the origin of this stability is unresolved, it is reasonable to consider π-donation (M−Ph) and allylic stabilization (M−allyl, M−benzyl) as factors in this result.[39] A recent paper has demonstrated the thermodynamic preference for benzylic C−H activation over β-C−H activation in a phenethyl ligand.[40] Another possible explanation for the curvature is that there is an ionic and/or electrostatic contribution to the bonding (*cf*., Drago's ECT parametrization of bond strengths[41]) when R = phenyl, allyl, and mesityl which is absent when R = alkyl. This component raises D(M−R) so these data points lie above the line in Figure 5. The upward curvature of this plot does support the notion that in a tradeoff between a hydrocarbon substrate and benzene (eq 1), *cleavage of the stronger C−H bond in benzene occurs due to the formation of the even stronger (rela-*

(36) For D(C−H) for benzene, see: Davico, G. E.; Bierbaum, V. M.; DePuy, C. H.; Ellison, G. B.; Squires, R. R. *J. Am. Chem. Soc.* **1995**, *117*, 2590−2599.

(37) D(C−H) for *tert*-butylethylene is based on the latest value of D(C−H) for ethylene. See: Ervin, K. M.; Gronert, S.; Barlow, S. E.; Gilles, M. K.; Harrison, A. G.; Bierbaum, V. M.; DePuy, C. H.; Lineberger, W. C.; Ellison, G. B. *J. Am. Chem. Soc.* **1990**, *112*, 5750−5759. For the other hydrocarbons, see footnote *a* in Table 3.

(38) Huang, J.; Haar, C. M.; Nolan, S. P.; Marshall, W. J.; Moloy, K. G. *J. Am. Chem. Soc.* **1998**, *120*, 7806−7815.

(39) Orbital-based rationalizations have been termed "popular...yet difficult to assess."[22] For an excellent discussion of the origin of stability, with consideration of covalent and ionic contributions to M−C bond enthalpies, sterics, and reaction coordination position see ref 22.

(40) Mak, K. W.; Chan, K. S. *J. Am. Chem. Soc.* **1998**, *120*, 9686−9687.

(41) Drago, R. S.; Wong, N. M.; Ferris, D. C. *J. Am. Chem. Soc.* **1992**, *114*, 91−98.

Table 3. Selectivities and Thermodynamics for the Formation of Tp′Rh(CNneo)(R)H (kcal/mol)[a]

R	D(C−H)[b]	k_{rel}(RH)[c]	$\Delta\Delta G_{oa}^{\ddagger}$ [c]	$\Delta G_{re}^{\ddagger}$ [d]	$\Delta G°$ [f]	D_{rel}(M−R)[g]
phenyl	113.5(5)[36]	1	0	30.99	0	0
HC═CHCMe$_3$	**109.7(8)[37]**	**10[c]**	**1.35**	**26.91[e]**	**5.31**	**9.3**
methyl	104.9(1)	2.3	0.43	23.52	7.90	16.5
n-pentyl	98	4.7	0.79	22.43	9.35	24.8
cyclopentyl	96.4(6)	24.8	1.65	21.18	11.46	28.6
cyclohexyl	96(1)	35.2	1.83	21.40	11.42	28.9
mesityl	88.5(1.5)	1.3	0.15	24.49	6.65	31.7
methallyl	**85.6(1.5)**	**4.3**	**0.75**	**23.92[d]**	**7.82**	**35.7**

[a] Values determined in the present study are given in boldface type. [b] Unless otherwise noted, bond strength values were obtained from: *CRC Handbook of Chemistry and Physics*, 78th ed.; Lide, D. R., Ed.; CRC Press: Boca Raton, FL, 1997. [c] $k_{rel} = k_{oa}(C_6H_6)/k_{oa}(RH)$ for oxidative addition of a molecule of substrate measured at −15 °C. [d] Measured at 23 °C. [e] Measured at 22 °C. [f] Relative to Tp′Rh(CNneo)(Ph)H. [g] Bond strengths relative to D(Rh−Ph) in Tp′Rh(CNneo)(Ph)H according to eq 4.

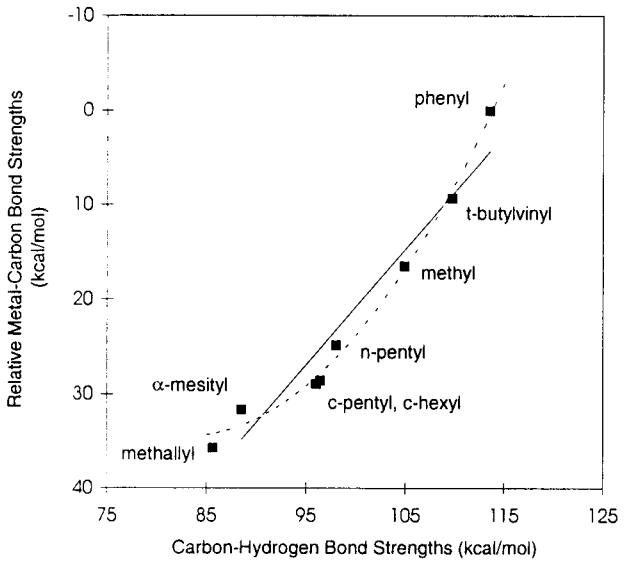

Figure 5. Plot of relative rhodium−carbon bond strengths vs carbon−hydrogen bond strengths for hydrocarbon substrates (slope of line 1.22). The dotted line is a least-squares parabolic fit.

tively) M−C bond. This trend is exactly the opposite for radical reactions, in which the weaker C−H bond yields the most stable radical species. Another useful feature of Figure 5 is that by considering a line of slope 1.0 passing through the data point for any individual substrate, all substrates lying above the line will be thermodynamically preferred over that substrate, while those below the line are less thermodynamically stable.

A comment should be made regarding the photolytic preparation of the vinyl hydride complex **1**, with regard to the kinetic selectivity of the fragment [Tp′Rh(CNneo)] for the C−H bond of ethylene. The ^{1}H NMR spectrum in C_6D_6 of the products from the photolysis of a cyclohexane solution of Tp′Rh(CNneo)(PhN═C═Nneo) under 2 atm of ethylene shows two major hydride-containing products in an approximate 2:1 ratio along with the usual small amount of carbodiimide activation products. The major product is the cyclohexyl hydride complex, and the minor product is **1**. The ratio of the cyclohexyl hydride to **1** was undoubtedly greater prior to exposure to C_6D_6, based on the basis of the half-life of the cyclohexyl hydride in C_6H_6, which is approximately 9 min at 23 °C. A more accurate ratio of the two species may be obtained by dividing the sum of the integral values for the neopentyl methyl protons of the cyclohexyl hydride and the phenyl-d_5 deuteride complexes by that of **1** and **2**. The ratio obtained in this manner is 4.8:1. A rough approximation of the selectivity of [Tp′Rh(CNneo)] for cyclohexane vs ethylene on a per-molecule basis is 0.22:1, which is calculated by multiplying the integral ratio (4.8) by the mole fraction of ethylene in *n*-hexane at 25 °C and 2 atm of partial gas pressure (0.046).[42] The selectivity for benzene to cyclohexane is 35.2:1, which, when multiplied by that for ethylene to cyclohexane, gives a benzene to ethylene selectivity ratio of 7.8:1. This is only a slightly lower selectivity ratio compared to the 10:1 ratio observed for benzene vs *tert*-butylethylene (vinylic C−H bond).

Conclusions

Photolysis of Tp′Rh(CNneo)(PhN═C═Nneo) in the presence of ethylene leads to activation of a vinyl C−H bond to produce the vinyl hydride complex **1**, in low yield. The vinyl hydride complex can be produced quantitatively from the reaction of the vinyl chloride complex and Cp_2ZrH_2 in C_6H_6. Photolysis of Tp′Rh(CNneo)(PhN═C═Nneo) in neat (−78 °C) propylene yields the allyl C−H bond activated product Tp′Rh(CNneo)($CH_2CH═CH_2$)H (**3**). Both hydrides are thermally unstable and rearrange to η^2-olefin complexes.

Photolysis of Tp′Rh(CNneo)(PhN═C═Nneo) in the presence of isobutylene and *tert*-butylethylene yields the first relatively stable allyl hydride (**5**) and vinyl hydride (**6**) complexes, respectively, for the present system. These complexes do not rearrange to η^2-olefin complexes, presumably due to the increased steric requirements of the substrates compared to ethylene and propylene. Both **5** and **6** reductively eliminate olefin in the presence of C_6H_6 to give Tp′Rh(CNneo)(C_6H_5)H. The rates of reductive elimination are first-order in metal complex in the presence of a large excess of C_6H_6.

Competition experiments between pairs of substrates, isobutylene vs *n*-pentane and *tert*-butylethylene vs benzene, have allowed for calculation of the kinetic selectivity of [Tp′Rh(CNneo)] for activation of allyl and vinyl C−H bonds, respectively, relative to a phenyl C−H bond. The selectivity for an allyl C−H bond is comparable to that for a primary C−H bond of *n*-pentane ($k_{benzene}/k_{isobutylene} = 4.3$). The selectivity of [Tp′Rh(CNneo)] for a phenyl C−H bond vs the *trans*-vinyl C−H bond of *tert*-butylethylene ($k_{benzene}/k_{tert-butylethylene} = 1.7$) is small. The steric effect of the *tert*-butyl group is to only permit one of the vinylic C−H bonds to be activated, but the reactivity of this bond is not significantly different from that of a C−H bond in ethylene. Combi-

(42) Wilhelm, E.; Battino, R. *Chem. Rev.* **1973**, *73*, 1−9.

nation of the reductive elimination data and the kinetic selectivity data has allowed for calculation of the free energy difference between Tp′Rh(CNneo)(C_6H_5)H and **5** (7.82 kcal/mol) and between Tp′Rh(CNneo)(C_6H_5)H and **6** (5.31 kcal/mol). The rhodium−carbon bond strengths, relative to the rhodium−phenyl bond strength, for **5** and **6** are calculated to be 35.7 and 9.3 kcal/mol, respectively. These values correlate with the trend that the stronger C−H bond of a hydrocarbon substrate yields a stronger M−C bond when activated by a coordinatively unsaturated transition-metal fragment. However, a strict linear correlation between Rh−R bond strengths and the corresponding R−H bond strengths is not obtained for complexes of the type Tp′Rh(CNneo)(R)H. Rather, a parabolic correlation is seen, the origin of which remains to be accounted for.

Experimental Section

General Considerations. All reactions, recrystallizations, chromatography, and routine manipulations, unless otherwise noted, were carried out at ambient temperature under a nitrogen atmosphere, either on a high-vacuum line using modified Schlenk techniques or in a Vacuum Atmospheres Corp. Dri-lab. All hydrocarbon solvents were distilled under nitrogen or vacuum from dark purple solutions of sodium benzophenone ketyl. Chlorinated solvents were distilled under vacuum from calcium hydride suspensions. Silica gel (200−400 mesh, 60 Å) for column chromatography was purchased from Aldrich Chemical Co. and dried under vacuum at 200 °C. Silica gel plates (2 mm) used in preparative thin-layer chromatography contained a fluorescent indicator and were purchased from Analtech.

Propylene (CP grade) and isobutylene (CP grade) were purchased from Matheson and J. T. Baker Co., respectively, and used as received. Neohexene (3,3-dimethyl-1-butene) was purchased from Aldrich Chemical Co., stirred over 4 Å Linde molecular sieves for 24 h, degassed using three freeze−pump−thaw cycles, and vacuum-transferred into an ampule with a Teflon-sealed vacuum line adapter. Carbon tetrachloride was purchased from Baker Chemical Co. and purified by the same method as that for neohexene. Methylene chloride, hexanes (for preparative TLC), and THF (for preparative TLC) were purchased from Fisher Chemical and used without further purification. The carbodiimide complex Tp′Rh(CNneo)(PhN=C=Nneo) was prepared according to a previously published procedure.[15] The vinyl chloride complex Tp′Rh(CNneo)(CH=CH_2)Cl was prepared as previously described.[26] Cp_2ZrH_2[43] and neopentyl isocyanide[44] were prepared as described in the literature.

All photolysis experiments and preparations were performed using a 200 W Hg(Xe) arc lamp purchased from Oriel. The light was filtered using a 345 nm long-pass quartz filter and water IR filter. Low temperatures were achieved with dry ice slurries of acetone (−78 °C) and methanol−water (−20 °C). ^{1}H (400 MHz) and ^{13}C (100 MHz) NMR spectra were recorded on a Bruker AMX-400 spectrometer. All chemical shifts are reported in ppm (δ) relative to tetramethylsilane and referenced to the chemical shifts of residual solvent resonances (C_6D_6, δ 7.15). Chemical shifts for ^{13}C NMR were measured in ppm relative to the deuterated solvent resonance (C_6D_6, δ 128.0). Resealable NMR tubes with Teflon valves were purchased from the Brunfeldt Co. Infrared spectra were recorded by a Mattson Instruments 6020 Galaxy Series FTIR and processed with First:Acquire v1.52 software. Elemental analyses were performed by Desert Analytics. A Siemens SMART (CCD) diffractometer was used for X-ray crystal structure determination of complex **6-Cl**.

Preparation of RhTp′(CNneo)(CH=CH_2)H (1). To a stirred solution of 5 mg (0.009 mmol) of RhTp′(CNneo)(CH=CH_2)Cl in 20 mL of C_6H_6 was added a suspension of 2 mg (0.009 mmol) of Cp_2ZrH_2 in 2 mL of C_6H_6. The reaction mixture was stirred for 30 min, giving a bright yellow suspension. Flash chromatography through a silica gel microcolumn, using 9:1 hexanes/THF as the eluant, followed by solvent evaporation gave a pale yellow oil. The yield of **1** was quantitative by ^{1}H NMR spectroscopy, but some conversion of **1** to the η^2-ethylene complex Tp′Rh(CNneo)(η^2-C_2H_4) (**2**) reduced the total amount of **1**. Upon standing at 22 °C, **1** was observed to convert quantitatively into **2**. Data for **1** are as follows. ^{1}H NMR (C_6D_6): δ −13.982 (d, J_{RhH} = 24 Hz, 1 H, RhH), 0.641 (s, 9 H, C(CH_3)$_3$), 2.188, 2.233, 2.300, 2.395, 2.565 (all s, 3 H, pzCH_3), 2.599 (bs, 5 H, NCH_2, pzCH_3), 5.602, 5.683 (both s, 1 H, pzH), 5.753 (dt, $J_{trans-HH}$ = 18 Hz, J_{gem-HH} = $^3J_{RhH}$ = 3 Hz, 1 H, *trans*-RhCHC*H*$_2$), 5.821 (s, 1 H, pzH), 6.210 (dtd, J_{cis-HH} = 10 Hz, J_{gem-HH} = $^3J_{RhH}$ = 3 Hz, $^4J_{H-hydride}$ (J_w) = 2 Hz, 1 H, *cis*-RhCHC*H*$_2$), 7.747 (ddd, $J_{trans-HH}$ = 18 Hz, J_{cis-HH} = 10 Hz, and $^2J_{RhH}$ = 3 Hz, 1 H, RhC*H*CH$_2$). Data for **2** are as follows. ^{1}H NMR (C_6D_6): δ 0.504 (s, 9 H, C(CH_3)$_3$), 2.163, 2.169 (both s, 3 H, pzCH_3), 2.325 (s, 6 H, pzCH_3), 2.342 (s, 2 H, NCH_2), 2.613 (s, 6 H, pzCH_3), 2.512 (bdd, J_{cis-HH} = 8 Hz, J_{gem-HH} = 2 Hz, 2 H, RhCH_2CH$_2$), 3.385 (bdd, J_{cis-HH} = 8 Hz, J_{gem-HH} = 2 Hz, 2 H, RhCH_2CH$_2$), 5.295 (s, 1 H, pzH), 5.890 (s, 2 H, pzH).

Preparation of Tp′Rh(CNneo)(CH_2CH=CH_2)H (3). Propylene (0.4 mL) was condensed at −78 °C into a resealable 5 mm NMR tube containing 5 mg (0.007 mmol) of Tp′Rh(CNneo)(PhN=C=Nneo). The resulting bright yellow solution was irradiated at −78 °C with λ >345 nm light until the carbodiimide complex had completely dissolved and the solution had become bleached (approximately 30−45 min). To aid solubilization at such low temperature, the sample was removed periodically from the cold bath, carefully agitated, and immediately returned to the cold bath. Excess propylene was removed at low temperature under high vacuum to give a pale brown-yellow solid. The yield was approximately 51% by ^{1}H NMR spectroscopy. The dominant minor product (19%) was the η^2-propylene complex Tp′Rh(CNneo)(η^2-H_2C=CHMe) (**4**), which was observed to increase over a 24 h period. Data for **3** are as follows. ^{1}H NMR (C_6D_6): δ −14.783 (d, J_{RhH} = 23 Hz, 1 H, RhH), 0.651 (s, 9 H, C(CH_3)$_3$), 2.284, 2.308, 2.356, 2.560, 2.611 (all s, 3 H, pzCH_3), 5.602, 5.629, 5.828 (all s, 1 H, pzH). Due to overlapping peaks the resonances for the remaining Tp′ methyl group, the methylene protons of the neopentyl isocyanide ligand, and all protons of the allyl ligand were not distinguishable. Data for **4** are as follows. ^{1}H NMR (C_6D_6): major product, δ 0.501 (s, 9 H, C(CH_3)$_3$), 2.166, 2.179, 2.305, 2.323, 2.621, 2.649 (all s, 3 H, pzCH_3), 5.302, 5.885, 5.916 (all s, 1 H, pzH); minor product, δ 0.416 (s, 9 H, C(CH_3)$_3$), 2.066, 2.109, 2.270, 2.377, 2.404, 2.413 (all s, 3 H, pzCH_3), 5.205, 5.885, 5.952 (all s, 1 H, pzH). Unassigned ^{1}H NMR resonances for the methylene protons of the neopentyl isocyanide ligand and all protons of the η^2-propylene ligand: δ 1.482 (dt, J = 8 Hz, 2 Hz), 1.952 (dd, J = 7 Hz, 2 Hz), 2.556 (s), 2.839 (bm), 2.920m (bd), 3.579 (bdt), 4.095 (bm), 4.227 (bm).

Preparation of Tp′Rh(CNneo)(CH_2CMe=CH_2)H (5). The method for preparing **5** was the same as that for **3**, except that isobutylene was used as the hydrocarbon solvent and the temperature for irradiation was −20 °C. The yield was 85% by ^{1}H NMR spectroscopy. The minor product was Tp′Rh(CNneo)H_2.[45] Data for **5** are as follows. ^{1}H NMR (C_6H_6, with solvent suppression): δ −14.661 (d, J_{RhH} = 23 Hz, 1 H, RhH), 0.672 (s, 9 H, C(CH_3)$_3$), 2.171 (s, 3 H, RhCH_2CCH_3CH_2), 2.187, 2.310, 2.373, 2.440, 2.583, 2.671 (all s, 3 H, pzCH_3), 2.813 (AB_q,

(43) Shriver, D. F. *Inorg. Synth.* Vol 19, 223−226.
(44) (a) Schuster, R. E. *Organic Synthesis*; Wiley: New York, 1973; Collect. Vol. 5, p 772. (b) Ugi, I.; Fetzer, U.; Eholzer, U.; Knupfer, H.; Offermann, K. *Angew. Chem., Int. Ed. Engl.* **1965**, *4*, 472−484.

2 H, NCH_2), 3.094 (AB_q d, J_{RhH} = 4 Hz, 2 H, $RhCH_2CCH_3CH_2$), 4.868 (bm, 1 H, $RhCH_2CCH_3CH_2$), 5.235 (bm, 1 H, $RhCH_2CCH_3CH_2$) 5.594, 5.632, 5.850 (all s, 1 H, pzH).

Synthesis of Tp′Rh(CNneo)(CH═CHCMe$_3$)(Cl) (6-Cl) *via* CCl_4 Quench of Tp′Rh(CNneo)(CH═CHCMe$_3$)H (6). To a 5 mL quartz tube containing a Teflon-coated magnetic stir bar and 60 mg (0.088 mmol) of Tp′Rh(CNneo)(PhN═C═Nneo) was added 2 mL of *tert*-butylethylene. The tube was sealed with a cap containing a valve and a vacuum line adapter. The resulting bright yellow solution changed to a dark yellow solution upon irradiation (λ >345 nm) for 30 min. Excess *tert*-butylethylene was removed under high vacuum to yield a dark yellow powder. A small sample of this powder was dissolved in C_6D_6. The yield of **6** was quantitative by ^{1}H NMR spectroscopy. Data for **6** are as follows. ^{1}H NMR (C_6D_6): δ −14.100 (d, J_{RhH} = 23 Hz, 1 H, RhH), 0.683 (s, 9 H, $C(CH_3)_3$), 1.227 (s, 9 H, $RhCHCHC(CH_3)_3$), 2.188, 2.243, 2.298, 2.396, 2.536, 2.568 (all s, 3 H, $pzCH_3$), 2.615 (AB_q, 2 H, NCH_2), 5.625, 5.692, 5.840 (all s, 1 H, pzH), 5.850 (dd, $J_{trans-HH}$ = 16 Hz, J_{RhH} = 2 Hz, 1 H, $RhCHCHC(CH_3)_3$). The vinyl proton of the rhodium-bound vinyl carbon was not observed due to overlapping resonances of free *N*-phenyl-*N*′-neopentylcarbodiimide in the region from δ 6.8 to 7.4.

The dark yellow solid was dissolved in 3 mL of hexanes and the solution cooled to −20 °C. Approximately 1 mL of CCl_4, chilled to −20 °C, was added all at once to the hexanes solution of **6**. The reaction mixture was kept in the dark at −20 °C for 24 h. The solution changed from yellow to green upon the addition of CCl_4. The solution volume was reduced, and the concentrate was purified by preparative TLC using 2:1 (v/v) hexanes/THF as the mobile phase. The lower band of only two bands was extracted with THF. This solution was filtered and evaporated to give 37 mg of crude **6-Cl** (69%) as a pale brown oil. Recrystallization from a solution of hexanes at −20 °C afforded pale brown-yellow microcrystals of analytical purity. Recrystallization by slow evaporation at ambient temperature in air of a 1:1 (v/v) CH_2Cl_2/hexanes solution gave pale green-yellow plates suitable for X-ray diffraction. ^{1}H NMR (C_6D_6): δ 0.761 (s, 9 H, $C(CH_3)_3$), 1.236 (s, 9 H, $RhCHCHC(CH_3)_3$), 2.101, 2.156, 2.240, 2.378, 2.822, 2.845 (all s, 3 H, $pzCH_3$), 2.615 (AB_q, 2 H, NCH_2), 5.579, 5.615, 5.732 (all s, 1 H, pzH), 5.913 (d, $J_{trans-HH}$ = 15 Hz, 1 H, $RhCHCHC(CH_3)_3$), 7.159 (dd, $J_{trans-HH}$ = 15 Hz, J_{RhH} = 3 Hz, 1 H, $RhCHCHC(CH_3)_3$). ^{13}C{^{1}H} NMR (C_6D_6): δ 12.29, 12.58, 12.86, 14.66, 15.34, 15.43 (all s, $pzCH_3$), 26.62 (s, $NCH_2C(CH_3)_3$), 31.95 (s, $NCH_2C(CH_3)_3$), 34.30 (s, $RhCHCHC(CH_3)_3$), 35.58 (s, $RhCHCHC(CH_3)_3$), 55.99 (s, NCH_2), 106.80, 107.64, 108.04 (all s, pzCH), 127.19 (d, J_{RhC} = 24 Hz, $RhCHCHC(CH_3)_3$), 142.70, 142.83, 144.26, 150.86, 151.51, 153.27 (all s, pzC_q). The resonance for C_β ($RhCHCHC(CH_3)_3$) of the vinyl carbons was not observed. IR (KBr): 2527 (B−H), 2214 , 2129 cm^{-1} (CNR). Anal. Calcd (found) for $C_{27}H_{44}BClN_7Rh$: C, 52.66 (52.84); H, 7.20 (7.33); N, 15.92 (15.79).

Kinetic Selectivity Experiments. Benzene and 3,3-Dimethyl-1-butene. A resealable 5 mm NMR tube was charged with 5 mg (0.008 mmol) of Tp′Rh(CNneo)(PhN═C═Nneo) along with 0.55 mL of a 4:1 (v/v) solution of *t*-butylethylen/C_6H_6 and 0.15 mL of C_6D_6. The tube was resealed and placed in the NMR probe at 22 °C. After careful shimming of the sample an initial ^{1}H NMR spectrum was acquired under standard conditions. The absolute frequencies of the solvent resonances were noted and entered into a frequency list which was part of a multiple solvent peak suppression program (UXNMR, zgh2mpr). A second spectrum using the suppression program was obtained to ensure that the routine was properly suppressing the solvent resonances. The sample was irradiated with λ >345 nm light for 7 min at 22 °C and was immediately placed in the NMR probe. Spectra with an acquisition time of 4 min were acquired every 10 min for 50 min to ensure that the integration ratios did not change substantially. An approach to thermal equilibrium was observed for the products after the sample had remained at 22 °C for 1 week.

Table 4. Summary of Crystallographic Data for 6-Cl

Crystal Parameters	
chem formula	$RhClN_7BC_{27}H_{44}$
fw	615.86
cryst syst	monoclinic
space group (No.)	$P2_1/c$ (14)
Z	4
a, Å	16.0413(7)
b, Å	11.0801(5)
c, Å	19.4294(8)
β, deg	113.1290(10)
V, Å^3	3175.8(2)
ρ_{calcd}, g cm^{-3}	1.288
cryst dimens, mm	0.02 × 0.05 × 0.20
temp, °C	−50
Measurement of Intensity Data	
diffractometer	Siemens SMART
radiation	Mo, 0.710 73
2θ range, deg	4.3−45.0
data collected	$-9 \le h \le 21$, $-14 \le k \le 14$, $-25 \le l \le 23$
no. of data collected	12 360
no. of unique data	4116
agreement between equiv data	0.062
no. of obsd data	2941 ($I > 2\sigma(I)$)
no. of params varied	346
μ, cm^{-1}	6.49
abs cor	empirical (SADABS)
range of transmissn factors	0.78−0.93
R1(F_o), wR2(F_o^2) ($I > 2\sigma(I)$)	0.0468, 0.0847
R1(F_o), wR2(F_o^2), all data	0.0829, 0.0970
goodness of fit	1.028

Pentane and Isobutylene. A resealable 5 mm NMR tube was charged with 5 mg (0.008 mmol) of Tp′Rh(CNneo)(PhN═C═Nneo) and resealed under nitrogen. The frozen sample was evacuated under high vacuum, and 2.3 mmol of isobutylene was condensed into the tube and subsequently frozen in liquid nitrogen. The sample was evacuated, and an equimolar amount of pentane was condensed into the tube. The sample was warmed to −78 °C to thaw the solvent mixture and was quickly placed in a resealable Pyrex Dewar that had been cooled to −15 °C with refrigerated nitrogen gas. The sample was irradiated (λ >345 nm) for 7 min, cooled to −78 °C, and evaporated to dryness under vacuum. Tetrahydrofuran-d_8 was condensed into the tube, and the tube was resealed. The sample was cooled to −78 °C and placed in a preshimmed, precooled NMR probe at −15 °C. Spectra with an acquisition time of 4 min were acquired every 10 min for 50 min to ensure that the integration ratios did not change substantially. It was not possible to observe the equilibration with isobutylene, since it had been removed from the sample.

Kinetics of Reductive Elimination of 5 in C_6H_6. A resealable NMR tube was charged with 10 mg (0.016 mmol) of Tp′Rh(CNneo)(PhN═C═Nneo), 0.4 mL of isobutylene was condensed into the tube at −20 °C, and the tube was resealed. The sample was photolyzed with λ >345 nm light until the bright yellow solution became completely bleached. Solvent was removed under vacuum, C_6H_6 was transferred into the tube, and the tube was resealed under partial pressure of benzene. The NMR probe (at 22 °C) was shimmed with a C_6D_6 sample of Tp′Rh(CNneo)(C_6D_5)D of concentration and solvent height similar to those of the experimental sample. The

(45) Wick, D. D. Ph.D. Thesis, University of Rochester, 1997. Data for Tp′Rh(CNneo)H_2 are as follows. ^{1}H NMR (C_6D_6): δ −14.530 (d, J_{RhH} = 21 Hz, 2 H, RhH_2), 0.610 (s, 9 H, $C(CH_3)_3$), 2.193 (s, 3 H, $pzCH_3$), 2.304 (s, 6 H, $pzCH_3$), 2.448 (s, 3 H, $pzCH_3$), 2.479 (s, 6 H, $pzCH_3$), 2.553 (s, 2 H, NCH_2), 5.553 (s, 1 H, pzH), 5.781 (s, 2 H, pzH). ^{13}C{^{1}H} NMR (C_6D_6): δ 12.56, 12.76, 15.43, 16.96 (all s, $pzCH_3$), 26.49 (s, $C(CH_3)_3$), 31.76 (s, $C(CH_3)_3$), 55.77 (NCH_2), 105.27, 105.32 (all s, pzCH), 143.24, 143.30, 149.35, 150.19 (all s, pzC_q). IR (C_6H_6): 2519 (B−H), 2166 (CNR), 2022 cm^{-1} (Rh−H). UV−vis (C_6H_6; λ, nm (ϵ, cm^{-1} M^{-1}): 294 (383).

UXNMR solvent suppression routine zgh2pr was used to acquire the ^{1}H NMR spectra. Between acquisitions the sample remained in a temperature-controlled room in which the monitored temperature fluctuated by no more than ± 2 °C. The hydride region was exclusively monitored, and the decrease in **5** over time was calculated by dividing the integral value of **5** by the sum of the integral values of **5** and Tp′Rh(CNneo)(C_6H_5)H.

Kinetics of Reductive Elimination of 6 in C_6H_6. An NMR tube containing a ground-glass joint and vacuum line adapter was charged with 10 mg (0.016 mmol) of Tp′Rh(CNneo)(PhN═C═Nneo) and 0.4 mL of *tert*-butylethylene. The joint was temporarily closed under an inert atmosphere, and the sample was irradiated (λ >345 nm) until the bright yellow solution became completely bleached (12 min). Solvent was removed under vacuum, C_6H_6 was transferred into the tube, and the tube was flame-sealed under vacuum. The NMR analysis was similar to that described for the reductive elimination of **5**.

X-ray Structural Determination of 6-Cl. Pale green-yellow plates were crystallized by evaporation at ambient temperature of a 1:1 (v/v) CH_2Cl_2/hexanes solution of **6-Cl**. A single crystal having approximate dimensions of 0.20 × 0.05 × 0.02 mm^3 was mounted on a glass fiber with epoxy. Data were collected at −50 °C on a Siemens SMART CCD area detector system employing a 3 kW sealed-tube X-ray source operating at 1.5 kW. A total of 1.3 hemispheres of data were collected over 13 h, yielding 2941 observed data after integration using SAINT (see Table 4). Laue symmetry revealed a monoclinic crystal system, and cell parameters were determined from 4135 unique reflections.[46] The space group was assigned as $P2_1/c$ on the basis of systematic absences using XPREP, and the structure was solved and refined using the SHELX95 package. For a Z value of 4 there is one independent molecule within the asymmetric unit. In the refinement model, non-hydrogen atoms were refined anisotropically (on F^2), with hydrogens included in idealized locations, with R1 = 0.0468 and wR2 = 0.0847.[47] Fractional coordinates and thermal parameters are given in the Supporting Information.

Acknowledgment is given to the U. S. Department of Energy (Contract No. FG02-86ER13569) for their support of this work.

Supporting Information Available: Figures giving plots of bond strengths and of linear free energies for the data in Table 3 and tables of crystallographic data, atomic coordinates, bond distances and angles, and anisotropic thermal parameters for **6-Cl**. This material is available free of charge via the Internet at http://pubs.acs.org.

OM9808211

(46) It has been noted that the integration program SAINT produces cell constant errors that are unreasonably small, since systematic error is not included. More reasonable errors might be estimated at 10× the listed values.

(47) Using the SHELX95 package, R1 = $(\sum||F_o| - |F_c||)/\sum|F_o|$ and wR2 = $\{\sum[w(F_o^2 - F_c^2)^2]/\sum[w(F_o^2)^2]\}^{1/2}$, where $w = 1/[\sigma^2(F_o^2) + (aP)^2 + bP]$ and $P = [f(\text{maximum of } 0 \text{ or } F_o^2) + (1 - f)F_c^2]$.